A broad-host-range CRISPRi toolkit for silencing gene expression in *Burkholderia*

Andrew M. Hogan[1], A. S. M. Zisanur Rahman[1], Tasia J. Lightly[1], Silvia T. Cardona[1,2*].

[1]Department of Microbiology, University of Manitoba, Winnipeg, MB, Canada.

[2]Department of Medical Microbiology & Infectious Disease, University of Manitoba, Winnipeg, Canada.

*To whom correspondence should be addressed: Silvia.Cardona@umanitoba.ca

Abstract

Genetic tools are critical to dissecting the mechanisms governing cellular processes, from fundamental physiology to pathogenesis. Members of the genus *Burkholderia* have potential for biotechnological applications but can also cause disease in humans with a debilitated immune system. The lack of suitable genetic tools to edit *Burkholderia* GC-rich genomes has hampered the exploration of useful capacities and the understanding of pathogenic features. To address this, we have developed CRISPR interference (CRISPRi) technology for gene silencing in *Burkholderia*, testing it in *B. cenocepacia*, *B. multivorans* and *B. thailandensis*. Tunable expression was provided by placing a codon-optimized *dcas9* from *Streptococcus pyogenes* under control of a rhamnose-inducible promoter. As a proof of concept, the *paaABCDE* operon controlling genes necessary for phenylacetic acid degradation was targeted by plasmid-borne sgRNAs, resulting in near complete inhibition of growth on phenylacetic acid as the sole carbon source. This was supported by reductions in *paaA* mRNA expression. The utility of CRISPRi to probe other functions at the single cell level was demonstrated by knocking down *phbC* and *fliF,* which dramatically reduces polyhydroxybutyrate granule accumulation and motility, respectively. As a hallmark of the mini-CTX system is the broad host-range of integration, we putatively identified 67 genera of Proteobacteria that might be amenable to modification with our CRISPRi toolkit. Our CRISPRi tool kit provides a simple and rapid way to silence gene expression to produce an observable phenotype. Linking genes to functions with CRISPRi will facilitate genome editing with the goal of enhancing biotechnological capabilities while reducing *Burkholderia'*s pathogenic arsenal.

Keywords

CRISPRi, *Burkholderia*, gene silencing, genetic tool

37

38 **Author contributions**

39 STC conceived the idea and design of the research; AMH designed and cloned the dCas9
40 constructs; AMH and ASMZ designed the sgRNAs, assessed knockdown phenotypes, processed
41 data, and wrote and edited the manuscript; TJL performed RT-qPCR analysis and edited the
42 manuscript; STC supervised the work and provided financial support.

43

44 **Graphical Abstract**

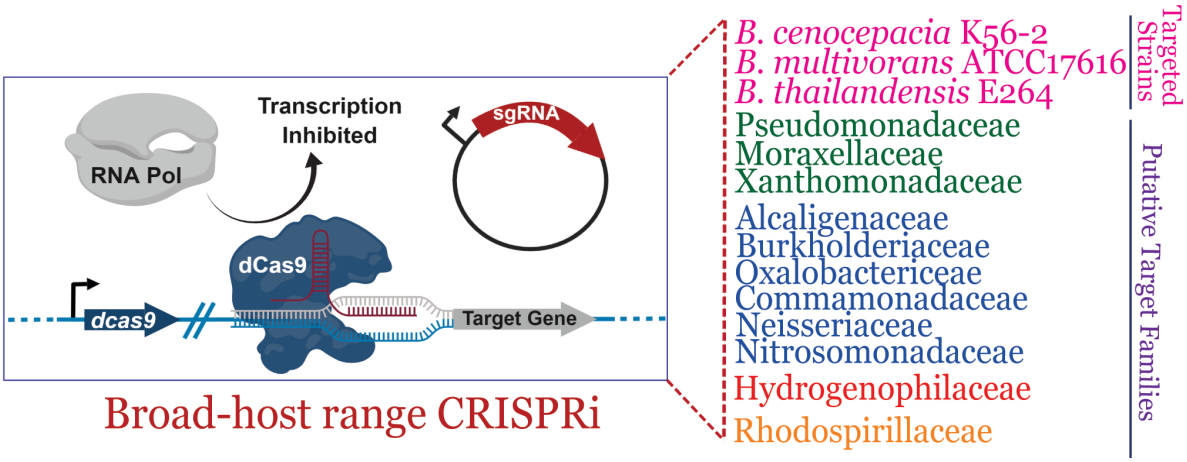

45

46

47 The genus *Burkholderia* comprises a diverse group of Gram-negative bacteria
48 characterized by a remarkable biotechnological potential, with species that can be exploited for
49 bioremediation purposes, production of bioactive compounds, and agricultural growth promotion.
50 Perhaps due to the phylogenetic diversity of the genus, some species of *Burkholderia* can also pose
51 a threat to human health [1]. Within the multiple deep-branching groups of the *Burkholderia*
52 phylogenetic tree [2], one branch contains the clades known as the *Burkholderia cepacia* complex
53 (Bcc) and the *B. pseudomallei* group. The Bcc group comprises species that cause severe infections
54 in people with the genetic disease cystic fibrosis and other patients with a compromised immune
55 system [3]. *B. cenocepacia* and *B. multivorans* are two relevant species of this group, which are
56 prevalent in cystic fibrosis patients [4]. The *B. pseudomallei* group contains the risk group 3 members
57 *B. mallei*, *B. pseudomallei*, and its close relative *B. thailandensis*, the last one being a frequent
58 surrogate used in *B. pseudomallei* and *B. mallei* research [5]. Other branches, such as the *B.*
59 *xenovorans* group comprise species isolated from diverse environmental sources, like polluted
60 soils, and plant rhizospheres [2]. While species with and without pathogenic potential tend to cluster
61 separately in most phylogenetic trees, the genetic characteristics that define the pathogenic
62 potential of *Burkholderia* are poorly understood. Environmental species can cause serious
63 infections [6], calling for caution in the use of *Burkholderia* strains for biotechnological applications.
64 The incomplete understanding of *Burkholderia* pathogenic potential may be related to the limited
65 tools available to link gene to function. Due to high resistance to the antibiotics typically used as
66 genetic markers [7], and the high GC content of their large genomes, most genome editing methods
67 designed for Gram-negative bacteria are inefficient and need to be adapted for use in *Burkholderia*.
68 Tools that facilitate controlled gene expression are necessary for interrogation of gene
69 function. Programmable control of gene expression by promoter replacement is a valuable tool to

70 link gene to phenotype [8]. Yet, promoter replacement implies that the natural regulatory circuitry
71 of the target gene is interrupted. Instead, clustered regularly interspaced short palindromic repeats
72 interference (CRISPRi) [9] is a method of silencing native gene expression, which is based on a dead
73 Cas9 (dCas9) and a nuclease-inactive version of the RNA-guided endonuclease Cas9 [10]. In
74 CRISPRi, a single guide RNA (sgRNA) designed towards the 5' end of the target gene and the
75 dCas9 protein form an RNA-protein complex that recognizes the target region by base-pairing,
76 and sterically blocks transcription initiation, if targeting the promoter, or elongation if targeting
77 downstream of the promoter, by the RNA polymerase [9]. Initially developed in *Escherichia coli*,
78 CRISPRi technology has been adapted to a wide range of bacterial strains to address focused
79 efforts such as metabolic rewiring and antimicrobial characterization [11–15], and broader efforts to
80 functionally characterize genomes [16–18]. To achieve fine control of gene expression, a wide range
81 of dCas9 expression levels are necessary, which can be provided by expressing *dcas9* with strong
82 inducible promoters [18] or by providing multiple copies of *dcas9* engineered in a plasmid [16].
83 Limitations to the success of these efforts are the proteotoxicity of dCas9 when expressed at high
84 levels [19] and the necessity of customizing CRISPRi delivery tools across bacteria. Recently, the
85 use of Tn*7* transposon mutagenesis, which specifically delivers genetic constructs close to a single
86 *glmS* site [20,21] was applied to deliver a mobile CRISPRi system across bacteria [22]. However, the
87 Tn*7* system is less suitable for *Burkholderia* species as their genomes contain multiple copies of
88 *glmS*, requiring additional steps to confirm the site of chromosomal integration [23].

89 In this work, we employ a mini-CTX-derived mutagenesis system [24] to achieve specific
90 chromosomal delivery of *dcas9* in three species of *Burkholderia*, *B. cenocepacia*, *B. thailandensis*
91 and *B. multivorans*. By placing the chromosomal copy of *dcas9* under the control of the *E. coli*
92 rhamnose-inducible promoter [25], we demonstrate durable and tunable control of endogenous gene

93 expression in *Burkholderia* species, which affects cellular function producing observable
94 phenotypes. We extend the usability of our CRISPRi tool kit by exploring other bacterial genomes
95 for putative mini-CTX insertion sites.
96

97 **Results**

98 *Construction of the CRISPRi system*

99 The dCas9 from *Streptococcus pyogenes* has been shown to provide robust gene repression
100 in diverse bacteria [9,18,22]; we therefore selected it as our first approach. To function, the dCas9
101 binds a sgRNA and, by complementary base pairing, is guided to target and silences a gene of
102 interest by sterically blocking the RNA polymerase [9]. However, the genome of *S. pyogenes* has
103 low GC-content (~40%), and from inspection of the *dcas9* gene, we expected poor codon usage in
104 high GC-content organisms such as *Burkholderia* (67%) and subsequently low levels of
105 expression. We first attempted to express the native gene from *S. pyogenes* in single copy in the
106 chromosome under control of the rhamnose-inducible promoter, which is known to yield robust
107 and tightly-regulated expression in *Burkholderia* [25]; however, we did not observe detectable levels
108 of dCas9 protein expression by immunoblot (Supplemental Figure 1). Upon codon optimization
109 for *B. cenocepacia*, we first introduced the gene into a multicopy plasmid under the control of the
110 rhamnose-inducible promoter [25]; however, we observed a severe growth defect upon induction,
111 except at minute concentrations of rhamnose (Supplemental Figure 2A). Growth inhibition was
112 not observed in the vector control (Supplemental Figure 2B) and it remains unclear if the inhibitory
113 effect of dCas9 expression on growth was caused by metabolic load from expression of a large
114 protein in multicopy, or from proteotoxicity [26].

115 A single chromosomal copy of *dcas9* may provide sufficient levels of expression as
116 observed previously [18,22,27]. Using the mini-CTX system, we introduced a single copy of *dcas9*
117 under control of the rhamnose-inducible promoter into *B. cenocepacia* K56-2 (Supplemental
118 Figure 3A and B). We observed titratable dCas9 expression at various levels of rhamnose by
119 immunoblot (Figure 1A and Supplemental Figure 4). At rhamnose concentrations up to 1% there
120 was no growth defect in K56-2::dCas9 (Figure 1B) or K56-2::dCas9 with non-genome targeting
121 sgRNA (pgRNA-non-target) (Figure 1C) compared to the vector control mutant (Figure 1D).

122 *Tunable and durable CRISPRi silencing of paaA suppresses growth on phenylacetic acid*

123 To evaluate the utility of the CRISPRi system for gene repression in *B. cenocepacia* K56-
124 2, we first chose to target the *paaA* gene, which encodes phenylacetate-CoA oxygenase subunit
125 PaaA [28]. This gene, and the rest of the *paaABCDE* operon, enable growth with phenylacetic acid
126 (PA) as a sole carbon source in *B. cenocepacia* K56-2 [29], with the lack of growth being a clearly
127 observable phenotype when the *paaA* gene is disrupted. In addition, as this is the first
128 characterization of CRISPRi in *Burkholderia*, we also wished to assess the effect on repression
129 efficiency when targeting the non-template (NT) and template (T) strands, as previous studies have
130 demonstrated profound differences [9,30]. We therefore designed five sgRNAs: three sgRNAs
131 targeted the promoter elements and adjacent to the transcription start site (TSS) on the NT strand
132 (sgRNA 1, 2 and 3), one sgRNA targeted near the start codon of *paaA* on the NT strand (sgRNA
133 4), and one sgRNA targeted near the start codon of *paaA* on the T strand (sgRNA 5) (Figure 2A).

134 For phenotypic characterization of the *paaA* mutants harbouring the codon-optimized
135 *dcas9*, we used M9 minimal medium with PA (M9+PA) as the sole carbon source. Upon induction
136 of dCas9, the growth of all mutants (except the controls) was suppressed approximately 30-fold
137 (Figure 2B) to the same level of a Δ*paaABCDE* mutant, which is unable to utilize PA as a sole

138 carbon source [29]. We observed only moderate repression (up to ~6-fold) when using the native
139 *dcas9* (Supplemental Figure 5). Furthermore, in the absence of rhamnose all of the mutants grew
140 at or near wild-type levels, suggesting that *dcas9* expression is tightly repressed in non-inducing
141 conditions. Phenotypically, we did not observe a differential effect of placement of the sgRNA-
142 binding site, as the growth of all mutants was suppressed equally. We also found there were no
143 differences in control strains; mutants expressing dCas9 and either a guideless or non-targeting
144 sgRNA displayed the same levels of growth. However, RT-qPCR demonstrated that while growth
145 was suppressed equally in the mutants, there were sgRNA-dependent differences in gene
146 expression levels (Figure 2C). At 0.2% rhamnose, sgRNA4, targeting near the start codon of *paaA*
147 on the NT strand, was the most effective in repressing *paaA* mRNA expression (at least 114-fold
148 repression), whereas sgRNA1 and sgRNA5 only had ~63-fold and ~51-fold repression,
149 respectively (Figure 2C). In the absence of rhamnose there was no difference in gene expression
150 levels between the mutants and wild type confirming that the *dcas9* is tightly regulated in non-
151 inducing conditions.

152 Next, we sought to determine the tunability of our CRISPRi system in *Burkholderia*.
153 Tuning is useful to control the level of transcriptional inhibition when precision is required, such
154 as in the study of essential genes. To that end, we examined the growth of the dCas9 mutant of *B.*
155 *cenocepacia* K56-2 with the sgRNA1 (targeting *paaA*), using PA as a sole carbon source in the
156 presence of various concentrations of rhamnose. The results showed that our CRISPRi system is
157 tunable, exhibiting growth reduction in a dose-dependent manner with variable repression across
158 sub-saturating rhamnose concentrations (between 0.005% and 0.05% rhamnose) (Figure 2D). This
159 trend was confirmed by RT-qPCR (Supplemental Figure 6). We observed a nearly 30-fold
160 repression in OD_{600nm} at concentrations well below maximum induction as identified by

161 immunoblot, suggesting our system produces more dCas9 than is required for maximum repression
162 as observed by this phenotype. Contrary to what had been observed in rich medium (Figure 1B
163 and C), all dCas9 mutants (with or without the sgRNA) showed a growth defect in M9+PA above
164 0.2% rhamnose (Figure 2D). A similar phenomenon was also seen in M9+glycerol (data not
165 shown). Intermediate levels of growth were observed in concentrations of rhamnose between
166 0.005% and 0.05%. For consistency, we therefore used 0.2% rhamnose for dCas9 induction in all
167 experiments.

168 Although once rhamnose is removed from the culture, expression of dCas9 is no longer
169 induced, it remained possible that the dCas9 already synthesized may persist and cause long-term,
170 or durable, silencing. To address this, the mutant strains harbouring sgRNAs targeting *paaA,* were
171 grown overnight in rich medium with 0.2% rhamnose, effectively priming the cells with dCas9.
172 Strikingly, when grown in M9+PA with and without rhamnose, we again observed strong
173 repression of growth (~30-fold) in all conditions regardless of the presence of rhamnose in the
174 M9+PA, and at levels similar to the Δ*paaABCDE* mutant (Figure 2E). This suggests that after the
175 inducer is removed, dCas9 is either slowly degraded in K56-2 or is present at high enough levels
176 in the cells for durable repression in growth inhibiting conditions. Moreover, the lack of growth is
177 not simply due to a loss in cell viability, as CFU/mL of the cultures did not decrease over time
178 (Supplemental Figure 7). We likely observed a durable knockdown in this scenario due to the
179 conditional essentiality of *paaA*. Due to the strong interaction of the dCas9:sgRNA complex with
180 its target, repression cannot be easily relieved except by the DNA polymerase machinery (Jones
181 et al. 2017). When transferred to medium with PA as the sole carbon source, cell growth would
182 halt from lack of a carbon source, therefore ensuring *paaA* expression remained repressed.

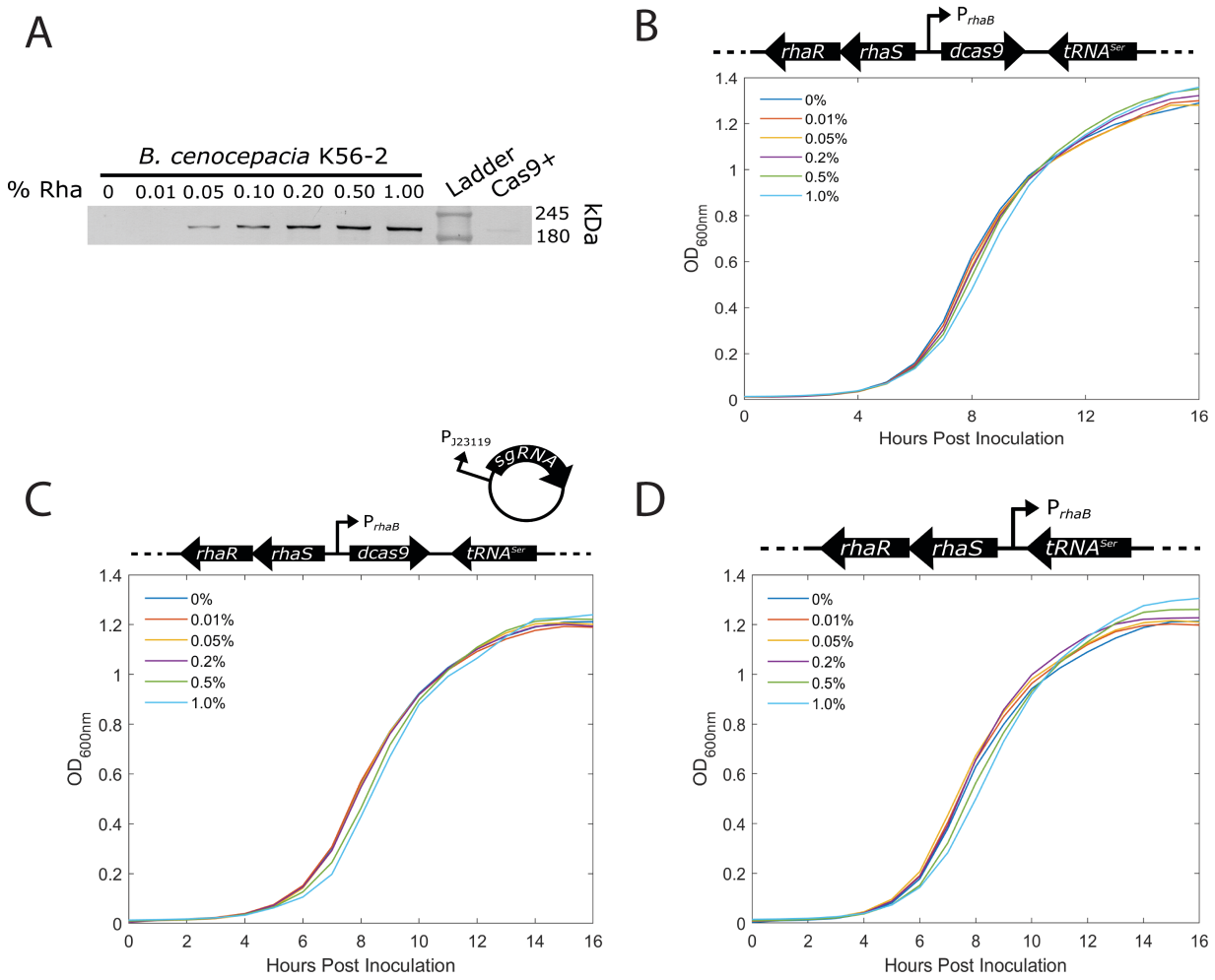

Figure 1. Development of CRISPRi in *B. cenocepacia* K56-2. A) dCas9 was expressed from the chromosome of K56-2 under a rhamnose inducible promoter. Cells were grown to OD_{600nm} of 0.6 then induced with rhamnose for three hours. The soluble protein fraction was run on an 8% SDS gel. dCas9 was detected by an α-dCas9 antibody followed by a second antibody linked to alkaline phosphatase. The lane labelled Cas9+ was loaded with 5 ng of purified Cas9. B, C and D) Growth curves of *B. cenocepacia* K56-2::dCas9 (B), dCas9 expressed with a non-genome targeting sgRNA (dCas9/pgRNA-non target) (C) and K56-2::CTX1-rha, the vector control plasmid for the integration (D) in LB media show that expression of the chromosomally-encoded dCas9 induced with rhamnose up to 1% does not affect growth.

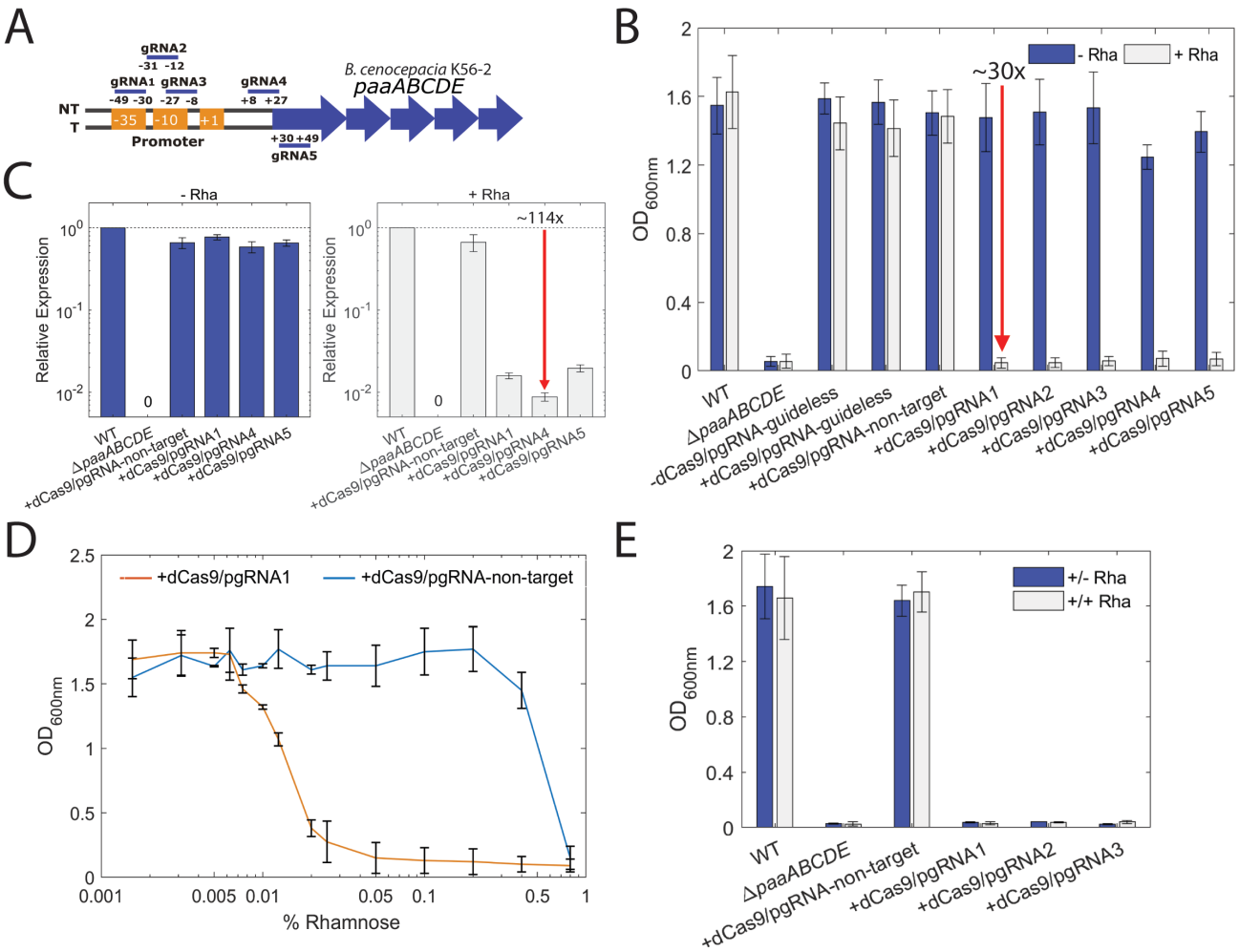

Figure 2. Targeting *paaA* with CRISPRi effectively suppresses growth in phenylacetic acid as the sole carbon source in *B. cenocepacia* K56-2. A) Positions of the sgRNAs targeting different regions upstream of and on *paaA*. sgRNAs 1, 2, and 3 were designed to target the promoter elements (-35 and -10 boxes) on the non-template (NT) strand. gRNA4 targeted the start codon on the NT strand and gRNA5 targeted the downstream region adjacent to the start codon on the T strand. B) CRISPRi blocks transcription in a strand non-specific manner. WT, a mutant of the *paaABCDE* operon (Δ*paaABCDE*), K56-2::CTX1-rha (-dCas9) and K56-2::dCas9 (+dCas9) harboring pgRNA with or without specific gRNAs were grown for 24 hours in minimal medium with PA (M9+PA) without (-Rha) or with 0.2% rhamnose (+Rha). C) RT-qPCR revealed a ~114-

204 fold reduction in paaA mRNA, demonstrating a robust knockdown of *paaA* expression in K56-2.
205 D) Expression of the dCas9 can be controlled by varying the amount of inducer added to the
206 medium, providing tunability to the CRISPRi system. However, high level induction of dCas9
207 with rhamnose (0.4% and beyond) was lethal for the non-genome targeting mutant
208 (dCas9/pgRNA-non-target) expressing dCas9. E) Cells were grown overnight in LB medium with
209 0.2% rhamnose to induce expression of dCas9. Then cells were transferred to M9+PA and grown
210 for 24 hours with (+/+ Rha) and without (+/- Rha) 0.2% rhamnose. All the values are the average
211 of three independent biological replicates; error bars represent arithmetic mean ± SD.

212

213

214 *Single-cell analysis reveals an 'all or none' effect in B. cenocepacia K56-2*

215 While at the culture level the effect of CRISPRi is tunable, we further explored the effect
216 of maximum dCas9 induction at the single-cell level. We therefore targeted *fliF,* a gene encoding
217 a transmembrane protein that forms both the S and M rings (MS ring) of the basal body complex
218 of the flagellum [31]. Silencing *fliF* should result in non-flagellated cells as FliF is required for
219 flagellum formation [32]. We targeted *fliF* by introducing four sgRNAs designed to bind near the
220 putative promoter and start codon on the NT strand (Supplemental Figure 8A). Our goal was to
221 assess individual cell flagellation and compare it with swimming motility at the population level.
222 While we observed an approximately 5-fold reduction in swimming motility compared to controls
223 in a plate-based assay (Supplemental Figure 8B and C), we were unable to observe flagella in any
224 of the mutants harbouring gRNAs targeting *fliF* (Supplemental Figure 8D). It is possible that
225 interfering with *fliF* expression rendered fragile flagella that could not remained attached to the
226 cell during the staining process, while still being functional when grown in culture [33]. In contrast
227 to the swimming motility of the CRISPRi mutants we confirmed that insertional inactivation of
228 *fliF* (*fliF*::pAH26) completely ablates swimming motility, as seen previously [34].

229 To further elucidate the effect of CRISPRi at the single cell level, we targeted *phbC,* a gene
230 encoding poly-β-hydroxybutyrate polymerase, an enzyme required for PHB synthesis. To repress
231 *phbC* expression, we designed three sgRNAs to target the region up to 50 bp before the start codon
232 on the NT strand, at the putative promoter site (Figure 3A). Polyhydroxyalkanoate (PHA) granule
233 accumulation was assessed by fluorescence microscopy with Nile Red staining after overnight
234 induction with rhamnose. For comparison to a null phenotype, we created a *phbC* insertional
235 mutant (*phbC*::pAH27) which was unable to produce PHA granules (Figure 3B and D). Compared
236 to the wild-type and non-target controls, markedly few cells harbouring sgRNAs targeting *phbC*

237 contained PHA granules, ranging from 17-70% depending on the sgRNA (Figure 3B). sgRNA6
238 rendered the strongest level of repression, with only 17.1% of cells containing PHA granules in
239 contrast to 86.9% for the wild-type (Figure 3B). Interestingly, although few cells possessed PHA
240 granules, the granules were of identical size to those in wild-type cells, averaging 0.65µm in
241 diameter (Figure 3C and 3D). As shown by the insertional mutant, inactivation of *phbC* ablates
242 PHA granule accumulation; therefore, the presence of granules of the same size in the dCas9
243 mutants as in the wild-type suggests an 'all-or-none' effect in *B. cenocepacia* K56-2, where most
244 cells display the silenced phenotype, but some manage to at least temporarily escape the effect of
245 CRISPRi.

246

247 *Broad host range of the mini-CTX system extends applicability to other species*

248 Having shown that the *S. pyogenes* dCas9 renders strong gene repression in *B. cenocepacia*
249 K56-2, we next turned our attention to other important species of *Burkholderia.* We introduced the
250 codon-optimized *dcas9* gene into the chromosome of *B. multivorans* ATCC 17616 and targeted
251 the *paaA* and *phbC* genes by designing three sgRNAs for each centered around the putative
252 promoter (Figures 4A and C). Targeted repression of *paaA* by each of the three sgRNAs strongly
253 suppressed growth in M9+PA by approximately 25-fold (Figure 4B), very similar to the activity
254 observed in *B. cenocepacia* K56-2. However, we were unable to detect robust expression of dCas9
255 by immunoblot in *B. multivorans* ATCC17616 (Supplemental Figure 9A) despite the observed
256 phenotype being indicative of expression of dCas9 and effective gene silencing. Expression of
257 dCas9 in the presence of the non-targeting sgRNA did not affect growth in *B. multivorans* ATCC
258 17616 (Supplemental Figure 9B). Following this, targeting

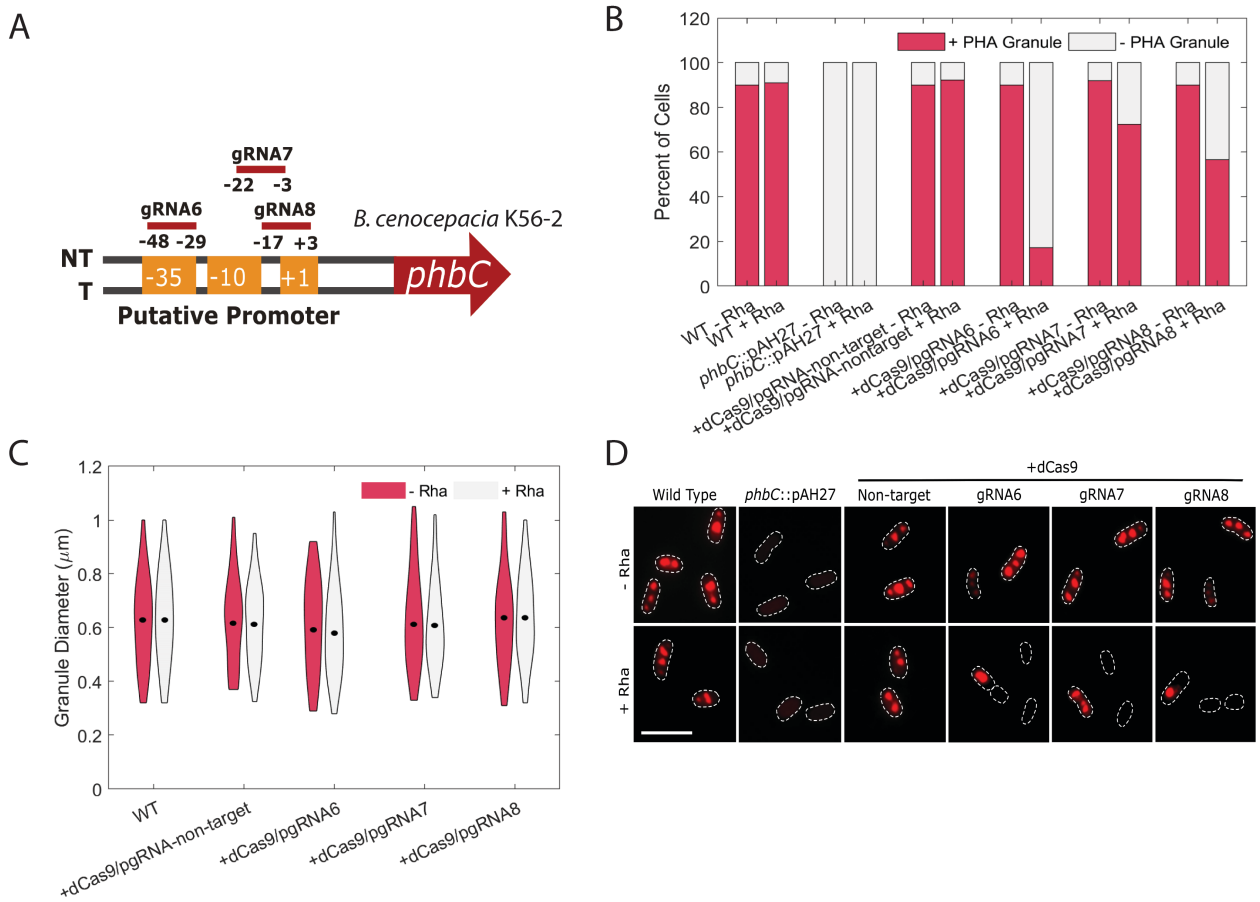

Figure 3. Targeting *phbC* with CRISPRi reduces polyhydroxyalkanoate (PHA) granule accumulation in K56-2. A) Positions of the sgRNAs targeting different regions upstream of *phbC*. sgRNAs 6, 7, and 8 were designed to target the promoter elements (-35 and -10 boxes) on the non-template (NT) strand. B) CRISPRi reduces but does not completely abrogate the number of cells with PHA granules. WT, an insertional mutant of the *phbC* gene (*phbC::*pAH27), K56-2::CTX1-rha (-dCas9) and K56-2::dCas9 (+dCas9) harboring pgRNA with or without specific gRNAs were grown overnight without (-Rha) or with 0.2% rhamnose (+Rha). Cells were washed and stained with Nile Red, and observed by fluorescence microscopy. One to two-hundred cells were counted and the % of cells with PHA granules was calculated. C) PHA granules that remain are identical to those in the WT. Strains were grown and processed as for B and the diameter of the PHA granules was measured. Thicker areas of the violin bars represent more granules with that diameter.

271 The mean in each condition is shown by a black dot. D) The strains were grown and processed as

272 for B). Dashes indicate cell boundaries and the scale bar is 5 μm.

273

274 *phbC* rendered relatively poor inhibition of PHA granule accumulation with between 35-50% of
275 cells containing PHA granules, depending on the sgRNA (Figure 4C and 4D). In contrast to what
276 was seen in *B. cenocepacia* K56-2, we observed granules of reduced size (Figure 4E and 4F).

277 Members of the *B. pseudomallei* group are phylogenetically distinct from the Bcc [1], but
278 remain of interest due to the ability to cause infection (such as melioidosis and glanders) and for
279 their remarkable capacity for secondary metabolite production [35]. *B. thailandensis* is a commonly
280 used model for the pathogenic members of the *B. pseudomallei* group, we therefore also introduced
281 the codon-optimized *dcas9* gene into the chromosome of *B. thailandensis* strain E264. When
282 induced with rhamnose, dCas9 was highly expressed (Supplemental Figure 9A) and did not impair
283 growth in the presence of a non-targeting sgRNA (Supplemental Figure 9B). Similarly, as for *B.*
284 *cenocepacia* K56-2 and *B. multivorans* ATCC 17616, we designed three sgRNAs targeting the
285 putative promoters of the *paaA* and *phbC* genes (Figure 5A and C). Upon induction of dCas9 with
286 0.2% rhamnose, growth of the mutants harbouring the *paaA*-targeting sgRNAs was suppressed in
287 M9+PA to varying levels ranging from 3-fold (sgRNA19) to 25-fold (sgRNA20) (Figure 5B).
288 Lastly, for the sgRNAs targeting *phbC*, the results mirror those seen in ATCC 17616, as depending
289 on the sgRNA there was variation in the percent of cells with PHA granules (10-40%) and the
290 diameter of the granules (overall decrease in size) (Figure 5C- F). Though the exact genetic
291 contributions to PHA synthesis in E264 remain unclear, it has been previously suggested that PhbC
292 is not the only polyhydroxyalkanoate polymerase in E264 [36].

293

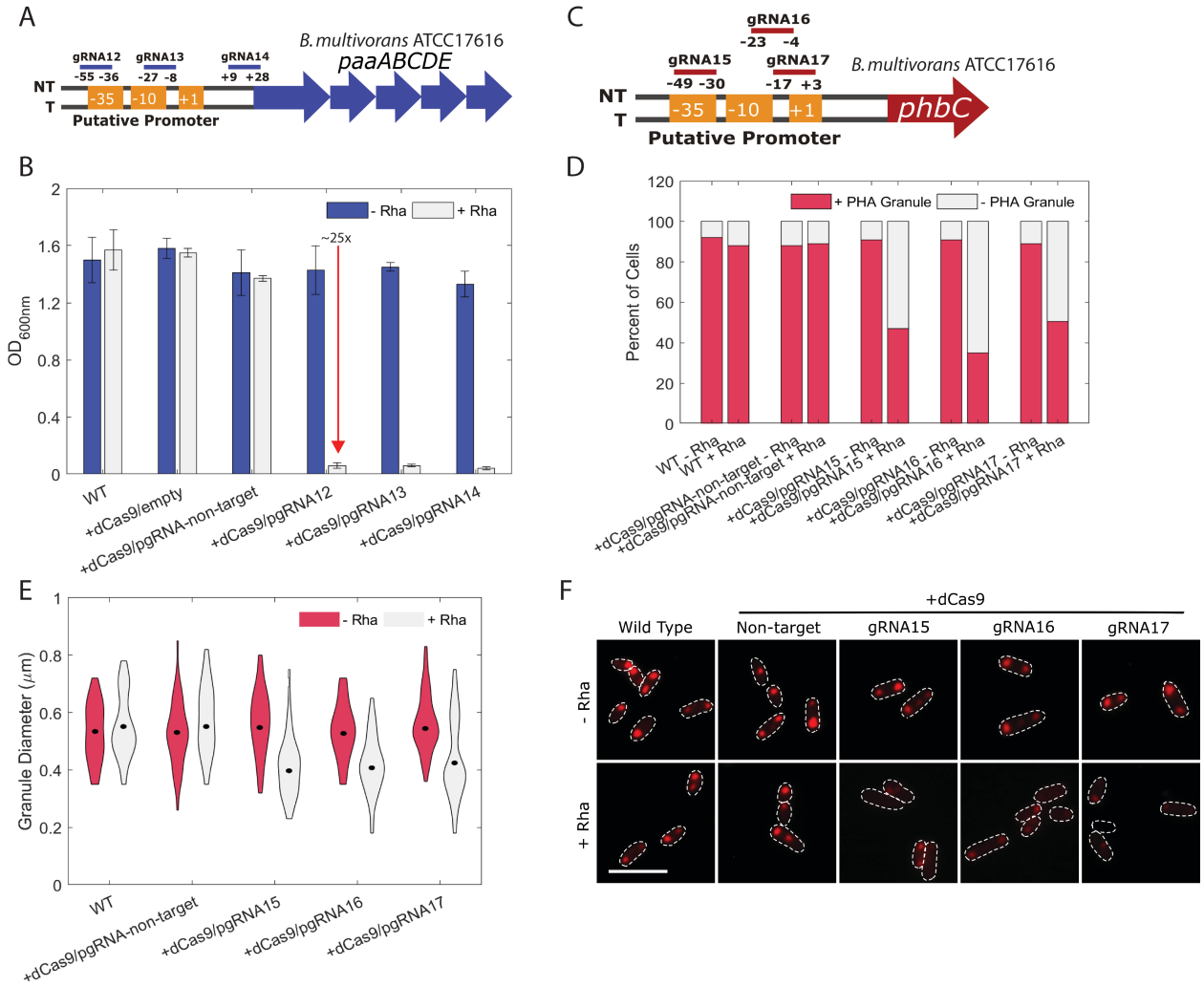

Figure 4. CRISPRi in *B. multivorans* ATCC17616 effectively represses *paaA* and *phbC*. A) Positions of the sgRNAs targeting upstream regions of *paaA*. sgRNAs12 and 13 were designed to target the -35 and -10 boxes of the promoter, while sgRNA14 targeted the 5' region of the ORF. All sgRNAs targeted the NT strand. B) Targeting *paaA* suppressed growth on PA as a sole carbon source. WT, ATCC 17616::dCas9 (+dCas9) with or without sgRNAs in A) were grown for 24 hours in M9+PA without (-Rha) or with 0.2% rhamnose (+Rha). C) Positions of the sgRNAs targeting upstream regions of *phbC*. All sgRNAs were designed to target the -35 or -10 elements of the promoter on the NT strand. D) Targeting *phbC* reduces the overall number of cells with PHA granules. Strains were grown overnight without (-Rha) or with 0.2% rhamnose (+Rha). Cells

304 were washed and stained with Nile Red, and observed by fluorescence microscopy. One to two-
305 hundred cells were counted and the % of cells with PHA granules was calculated. E) PHA granules
306 that remain are smaller than those in the WT. Strains were grown and processed as for D); however,
307 the diameter of the PHA granules was measured, with thicker areas representing more granules
308 with that diameter. The mean in each condition is shown by a black dot. F) The strains were grown
309 and processed as for D). Dashes indicate cell boundaries and the scale bar is 5 μm.

310

311

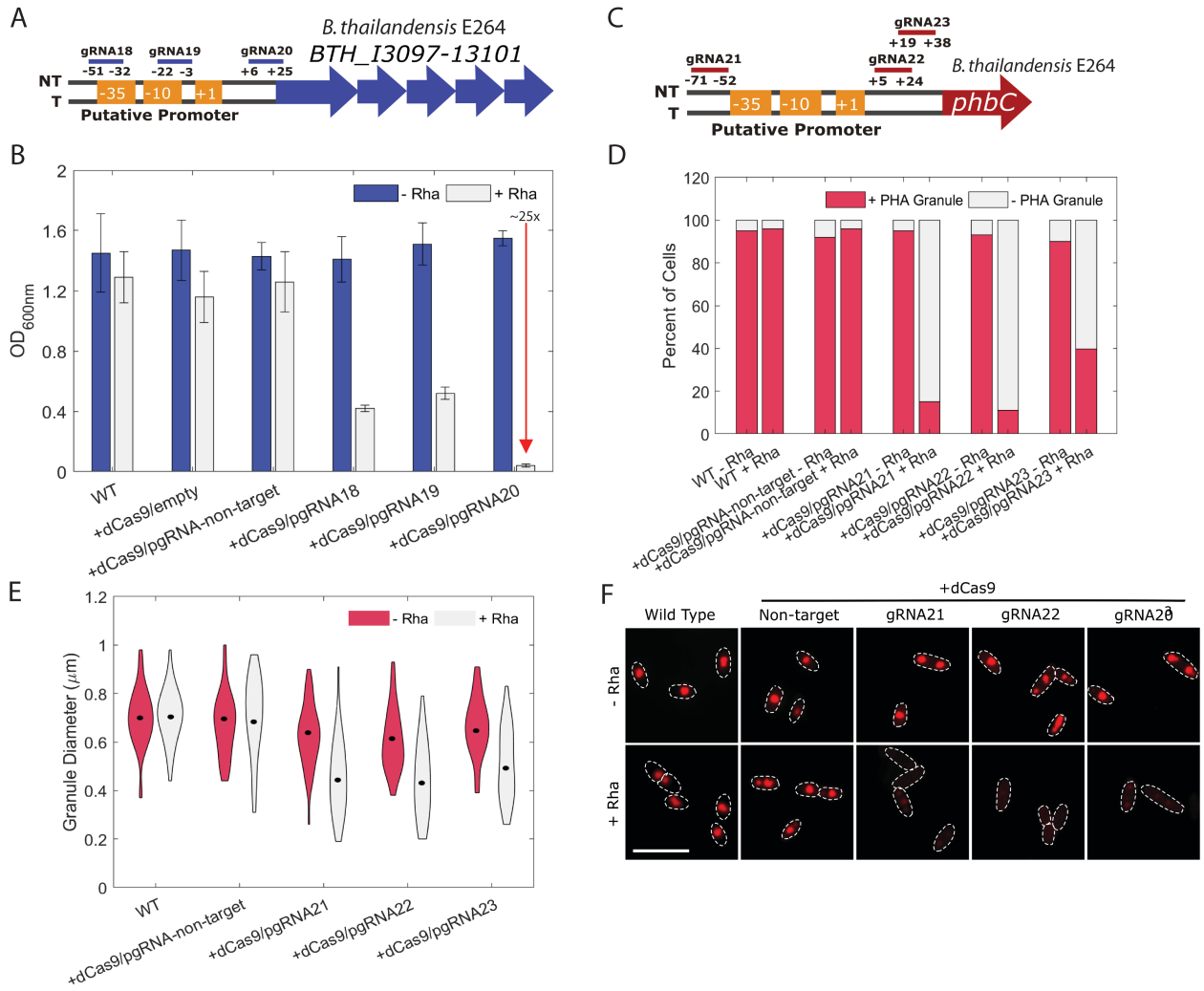

Figure 5. CRISPRi in *B. thailandensis* E264 effectively represses *paaA* (BTH_I3097) and *phbC*. Positions of the sgRNAs targeting upstream regions of *paaA* (BTH_I3097). sgRNAs 18 and 19 were designed to target the -35 and -10 boxes of the promoter, while sgRNA 20 targeted the 5' region of the ORF. All sgRNAs targeted the NT strand. B) Targeting *paaA* suppressed growth on PA as a sole carbon source. WT, E264::dCas9 (+dCas9) with or without sgRNAs in A) were grown for 48 hours in M9+PA without (-Rha) or with 0.2% rhamnose (+Rha). C) Positions of the sgRNAs targeting regions of *phbC*. sgRNA 21 targeted just upstream of the -35 box, sgRNA22 and 23

321 targeted just downstream of the -10 box, all on the NT strand. D) Targeting *phbC* reduces the
322 overall number of cells with PHA granules. Strains were grown overnight without (-Rha) or with
323 0.2% rhamnose (+Rha). Cells were washed and stained with Nile red, and observed by
324 fluorescence microscopy. One to two-hundred cells were counted and the % of cells with PHA
325 granules was calculated. E) PHA granules that remain are smaller than those in the WT. Strains
326 were grown and processed as for D); however, the diameter of the PHA granules was measured,
327 with thicker areas representing more granules with that diameter. The mean in each condition is
328 shown by a black dot. F) The strains were grown and processed as for D). Dashes indicate cell
329 boundaries and the scale bar is 5 μm.
330

331 The integration vector we implemented to deliver *dcas9* to the chromosome of various
332 species of *Burkholderia* relies on the expression of the φCTX integrase and recombination using
333 the plasmid-borne *attP* site with the chromosomal *attB* site [24]. φCTX is a *Pseudomonas*-infecting
334 phage, and the mini-CTX integration system was originally designed for use in *P. aeruginosa* [24].
335 The mini-CTX integration system has been used successfully in other species; however, this has
336 been mostly limited to members of *Burkholderia* [37,38]. The utility in *Burkholderia* has been
337 comparable to *P. aeruginosa*, in part owing to efficient integration. In the species used in this
338 study, we observed the integration efficiencies to be $6x10^{-7}$ in K56-2, $6x10^{-8}$ in E264, and $5x10^{-9}$
339 in ATCC 17616 (Supplemental Figure 10A), compared to 10^{-7} to 10^{-8} observed previously in *P.*
340 *aeruginosa* [24]. To further broaden the scope of the applicability of our CRISPRi system, we used
341 NCBI BLAST to search all published genomes for putative *attB* sites. While the full-length *attB*
342 site is 30 nt, integration is known to occur if only the 5' 19 nt are completely complementary, such
343 as for many species of *Burkholderia*. This shorter *attB* site was therefore used as a BLAST query,
344 resulting in 1760 hits with 100% alignment (Supplementary Table 5). Enterobacteria were
345 excluded from the search as the pMB1 *oriR* in the mini-CTX system is functional is these species;
346 therefore, integrants cannot be easily isolated. Furthermore, the search parameters were modified
347 to only include species of Proteobacteria, as there were few hits of non-Proteobacterial species
348 with 100% alignment (data not shown). Overall, there were 168 unique species from 67 genera.
349 As expected, the most abundant hit corresponded to species and strains of *Pseudomonas* (480 hits),
350 then followed by *Acinetobacter* (443 hits), *Burkholderia* (276 hits), *Neisseria* (170 hits), and
351 *Ralstonia* (146 hits), with members of the other 62 genera comprising the remaining 245 hits. A
352 summary of the major hits and species of interest (pathogenic, environmental, biotechnological,
353 etc.) can be found along with the genomic context in Table 1. We note that the hit table comprises

354 species with both high and low GC-content genomes, and while the GC-rich codon-optimized
355 *dcas9* (in pAH-CTX1-rhadCas9) may be better suited for species with high GC-content genomes,
356 such as those in the families *Pseudomonadaceae* and *Alcaligenaceae*, the native *dcas9* (in pAH-
357 CTX1-rhadCas9-native) may have better functionality in species with low GC-content genomes,
358 such as those in the families *Moraxellaceae* and *Neisseriaceae*.

359 A further consideration for use of our CRISPRi system is that the pFLPe recombinase-
360 expressing plasmids might not be functional in all species. In which case, the *int* gene along with
361 the *oriT*, pBM1 *oriR,* and the *tet* gene would not be excised. Continued expression of the integrase
362 could cause instability of the integrated DNA and loss of the dCas9 gene over time. To explore
363 this possibility, we assessed the stability of the mini-CTX integration in K56-2, ATCC 17616, and
364 E264 in serial passages over four days without tetracycline selection. For all species over the entire
365 experiment we determined CFU counts on agar with and without tetracycline selection and found
366 equal recovery of tetracycline-resistant colonies as total colonies (Supplemental Figure 10B-D),
367 suggesting the integration containing the dCas9 is stable.

368 **Table 1.** Putative host range of the mini-CTX system and genomic context of selected hit sites

Class	Order	Family	Genus and Species	Strain	%GC	tRNA^{Ser} ( ) Genomic Context
Gammaproteobacteria	Pseudomonadales	Pseudomonadaceae	*Pseudomonas aeruginosa*	PAO1	66.6	PA2603 PA2603.1 PA2604
			Pseudomonas fluorescens	NCTC 10783	65.9	EL286_RS07725 EL286_RS07730 EL286_RS07735
			Pseudomonas mendocina	NK-01	64.7	MDS_RS12060 MDS_RS12065 MDS_RS12070
		Moraxellaceae	*Acinetobacter baumannii*	ATCC 17978	39	AUO97_RS02215 AUO97_RS02215 AUO97_RS02220 fadH AUO97_RS12570 AUO97_RS12570
			Acinetobacter nosocomialis	NCTC 8102	38.7	DIW83_RS04465 DIW83_RS04470 DIW83_RS04475 DIW83_RS13465 DIW83_RS13470 fadH
	Xanthomonadales	Xanthomonadaceae	*Xylella fastidiosa*	M12	51.9	XFASM12_RS11770 XFASM12_RS07835 XFASM12_RS07840
Betaproteobacteria	Burkholderiales	Alcaligenaceae	*Achromobacter xylosoxidans*	NCTC 10808	67.4	DQO23_RS06440 DQO23_RS06445 DQO23_RS06450
			Bordatella bronchiseptica	D448	68.1	CS344_RS23895 CS344_RS23900 CS344_RS23905
			Alcaligenes faecalis	DSM 30030	56.6	CPY64_RS11990 CPY64_RS11995 CPY64_RS12000
		Burkholderiaceae	*Ralstonia pickettii*	DTP0602	65.9	N234_04430 N234_04435 N234_04440
			Burkholderia cenocepacia	K56-2	67	WQ49_RS02320 WQ49_RS02325 WQ49_RS02330
			Burkholderia multivorans	ATCC 17616	66.7	BMULJ_RS32145 BMULJ_RS04140 BMULJ_RS04145
			Burkholderia thailandensis	E264	67.7	BTH_RS32930 BTH_RS20275 BTH_RS20280
			Burkholderia mallei	NCTC 10229	68.5	BMA10229_RS30760 BMA10229_RS21960 BMA10229_RS21965
			Burkholderia pseudomallei	NCTC 13178	67.9	BBJ_RS32360 BBJ_RS01310 BBJ_RS01315
			Burkholderia oklahomensis	EO147	66.9	DM82_RS11255 DM82_RS11260 DM82_RS11265
			Cupriavidus necator	NH9	65.5	BJN34_RS05080 BJN34_RS05085 BJN34_RS05090
			Pandoraea apista	AU2161	62.6	AA956_RS16715 AA956_RS16720 AA956_RS25505
			Lautropia mirabilis	NCTC 12852	65.5	EL249_RS10610 EL249_RS10615 EL249_RS10620
		Oxalobactericeae	*Collimonas fungivorans*	Ter6	59	CFter6_RS10510 CFter6_RS10515 CFter6_RS25055
		Commamonadaceae	*Rhodoferax antarcticus*	DSM 24876	58.9	RA876_RS18910 RA876_RS18915 RA876_RS18920
			Polaromonas naphthalenivorans	CJ2	61.7	PNAP_RS04840 PNAP_RS04845 *ureG*
	Neisseriales	Neisseriaceae	*Neisseria meningitidis*	NCTC 10026	51.4	EL323_RS06235 EL323_RS06240 *yaaA*
			Neisseria gonorrheae	NCTC 13484	52.5	EL177_RS06240 EL177_RS06245 *yaaA*
			Neisseria sicca	FDAARGOS_260	50.9	A6J88_RS26510 A6J88_RS26515 A6J88_RS26520
			Chromobacterium violaceum	CV1197	65.6	CR207_RS10565 CR207_RS10570 CR207_RS10575
	Nitrosomonadales	Nitrosomonadaceae	*Nitrosomonas communis*	Nm2	44.7	AAW31_RS16120 AAW31_RS16125 AAW31_RS16130
Hydrogenophilalia	Hydrogenophilales	Hydrogenophilaceae	*Hydrogenophilus thermoluteolus*	TH-1	61.7	HPTL_RS08770 HPTL_RS08775 HPTL_RS08780
Alphaproteobacteria	Rhodospirillales	Rhodospirillaceae	*Haematospirillum jordaniae*	H5569	55.6	AY555_RS08435 AY555_RS08440 AY555_RS08445

369

370 **Discussion**

371 Genetic tools are necessary to dissect the molecular mechanisms governing cellular
372 processes. Here, we report the development of a CRISPRi system for efficient repression of gene
373 expression in *Burkholderia*. By mobilizing the *dcas9* gene that was codon-optimized for the GC-
374 rich *Burkholderia* on a broad host range mini-CTX1 integration vector, we demonstrate robust,
375 tunable, and durable repression of endogenous genes. While others have shown effective
376 repression using the native *dcas9* gene in *E. coli* [9], *B. subtilis* [18], *Staphylococcus aureus*, and
377 *Acinetobacter baumannii* [22], codon-optimization was a necessary step for K56-2, as expression of
378 the native *dcas9* gene was not detectable in K56-2. Indeed, for expression in species with high
379 GC-content, codon optimization appears to be necessary. In *P. aeruginosa* (66.3% GC) both the
380 *S. pyogenes* dCas9 [22] and the *S. pasteurianus* dCas9 [13] were not expressed unless first codon-
381 optimized, albeit for *Homo sapiens* (optimized at 50.2% GC) or *Mycobacterium* (~67% GC),
382 respectively. Additionally, the *S. thermophilus* dCas9 was codon-optimized for *Mycobacterium*
383 for efficient expression in *M. tuberculosis* and *M. smegmatis* [26].

384 Upon codon-optimizing the *dcas9* gene, we observed a severe growth defect when
385 expressed from a multicopy pBBR1-origin plasmid. At this time, we are unsure if this was caused
386 by a metabolic burden of expressing a large protein from a multicopy plasmid or from direct
387 proteotoxicity. Previous studies have demonstrated that expression of the canonical *S. pyogenes*
388 dCas9 causes toxicity in *M. smegmatis*, *M. tuberculosis* [26], and *E. coli* [39], which provides rationale
389 for developing a system with low-enough levels of dCas9 expression to maintain cell viability
390 without sacrificing repression activity. While this effort has spurred the exploration of alternative
391 dCas9 orthologues [26], we found that introducing *dcas9* in single copy in the chromosome provided
392 a balance of repression activity without affecting growth. Furthermore, while other systems display

393 up to 3-fold repression in the absence of inducer [13,18], our application of the tightly regulated
394 rhamnose-inducible promoter from *E. coli* did not display a leaky phenotype in any of the three
395 species tested. While we did observe increased dCas9 expression at rhamnose concentrations of
396 0.5% and 1.0% with no inhibitory effect on growth in LB (Figure 1C and D), the increased level
397 of dCas9 expression was accompanied by a substantial growth defect in M9 minimal media with
398 PA (Figure 2D) or glycerol (data not shown) as the sole carbon source. As the growth rate is
399 decreased in minimal media, it is possible that growth inhibitory, off-target effects that are
400 alleviated in fast growing cells by dilution of dCas9 bound DNA sites with newly replicated ones,
401 are more evident in slowly growing cells. While the RNA polymerase is largely incapable of
402 displacing the dCas9:sgRNA complex, the DNA replication machinery is not blocked by dCas9.
403 In fact, it has been observed that the dissociation of the dCas9:sgRNA complex correlates well
404 with the generation time in *E. coli* [40]. This is an important consideration for understanding the
405 durability of growth suppression we observed when using PA as a sole carbon source. Cells primed
406 by pre-incubation with rhamnose are unable to grow in M9+PA, creating a condition where *paaA*
407 is an essential gene and its absence would arrest cell division and replication. Hence, the DNA
408 replication machinery would not displace the dCas9:sgRNA from the *paaA* gene, resulting in long-
409 term growth suppression. By extension, we predict that strong knockdown of any (conditionally)
410 essential gene that causes a halt in DNA replication would be durable in this manner. This is a
411 useful aspect of CRISPRi that we are investigating further.

412 Although it has been reported that the CRISPRi system is less effective in silencing gene
413 expression when the template strand (T) is targeted compared to the non-template (NT) strand, our
414 results demonstrated nearly 30-fold suppression of growth irrespective of the *paaA* target strand
415 (Figure 2B). This suggests that the efficiency of the CRISPRi system might not be strand specific

416 at all loci, supporting the findings from Guo et al. [41]. However, this effect might have been masked
417 by the strong repression we observed, as it is difficult to compare across null phenotypes. Our
418 findings are also supported by the RT-qPCR that demonstrated differential repression of gene
419 expression based on the targeted location. Interestingly, our data suggests that, for *paaA,* targeting
420 near the start codon of the NT strand (gRNA4) was more effective than targeting near the start
421 codon of the T strand (gRNA5). Additionally, sgRNAs targeting different regions of the 5' region
422 of *paaA* produced a strong 25 to 30-fold repression in the three species studied here. Therefore,
423 the observed knockdown efficiency appears to be largely unaffected by sgRNA placement on
424 targeting regions overlapping or adjacent to the −35 and −10 promoter elements, at least for
425 phenotypes where complete repression of gene expression is not required. The cause of this is
426 likely due to the large dCas9:sgRNA complex that when bound to the promoter sterically interferes
427 with RNA polymerase binding. Indeed, the ~160 kDa dCas9 enzyme has an average DNA footprint
428 of 78.1 bp, much larger than most promoter regions [42]. This could explain why Cui et al. [19], and
429 our results for *paaA*, demonstrate strong repression when the template strand is targeted a short
430 distance downstream of the transcription start site.

431 Single cell level analysis of our system suggested a unimodal 'all or none' effect in K56-2
432 with ~17% cells escaping the silenced phenotype when targeting *phbC* compared to an insertion
433 mutant, which did not possess any PHA granules. The PHA granules in these cells were of identical
434 diameter to wild type. The 'all or none' effect might be attributed to an uneven distribution of
435 sugar transporters after cell division as observed previously for arabinose-inducible expression [43].
436 If a similar mechanism involved transporting rhamnose into the cell, some cells could escape the
437 rhamnose-mediated *dcas9* induction to silence the target gene. We hypothesize any escape would
438 be temporary as the transporter would be expressed in growing cells, allowing rhamnose uptake.

439 However, a rhamnose transporter in *Burkholderia* has so far not been described. Interestingly,
440 targeting *phbC* in *B. multivorans* ATCC17616 and *B. thailandensis* E264 resulted in a mixed
441 phenotype with a reduced number of cells with granules as well as an overall decrease in granule
442 size. Even though some of the cells appeared to have escaped the repression (up to 35% in
443 ATCC17616 and 6% in E264), more than 90% of the cells contained granules of reduced size.
444 This suggests that there is an unelucidated secondary PHA synthesis pathway in *B. thailandensis*
445 E264 and *B. multivorans* ATCC17616. Funston et al. [36] have observed similar results in *B.*
446 *thailandensis* E264 where transposon mutants in *phb* genes (*phbA*, *phbB* and *phbC*) retained the
447 ability to synthesize PHA, albeit at lower levels.

448 One of the hallmarks of CRISPRi is the broad-range amenability in diverse bacteria,
449 enabling synthetic biology and mechanistic investigations into many dozens of species in
450 innovative ways. We wished to apply our CRISPRi system in this manner and therefore mobilized
451 both the native *dcas9* gene, suitable for low/medium GC-content organisms, and the *dcas9* gene,
452 codon-optimized for GC-rich *Burkholderia*, on the mini-CTX1 integration vector. Our analysis of
453 putative hosts (with *attB* sites near the 3' end of the serine tRNA) identified 168 unique species in
454 67 genera, mostly from the β- and γ-Proteobacteria. Previous works have mobilized *dcas9* on
455 broad host-range integrative plasmids [13,22]; however, both systems use the mini-Tn*7* system, which
456 has multiple insertion locations in certain genomes, such as many species of *Burkholderia*.
457 Together, our work contributes to the available genetic toolkit for rapid functional analysis of
458 bacteria.

459

460

461 **Methods**

462 *Strains, selective antibiotics, and growth conditions*

463 All strains and plasmids are found in Supplemental Table 1. All strains were grown in LB-
464 Lennox medium (Difco). *B. cenocepacia* K56-2 and strains of *E. coli* were grown at 37°C, while
465 *B. thailandensis* E264 and *B. multivorans* ATCC 17616 were grown at 30°C. The following
466 selective antibiotics were used: chloramphenicol (Sigma; 100 µg/mL for *B. cenocepacia,* 20
467 µg/mL for *E. coli*), trimethoprim (Sigma; 100 µg/mL for strains of *Burkholderia*, 50 µg/mL for *E.*
468 *coli*), tetracycline (Sigma; 50 µg/mL for all strains of *Burkholderia*, 20 µg/mL for *E. coli*),
469 kanamycin (Fisher Scientific; 250 µg/mL for *B. thailandensis*, 150 µg/mL for *B. multivorans*, 40
470 µg/mL for *E. coli*), ampicillin (Sigma; 100 µg/mL for *E. coli*), gentamicin (Sigma; 50 µg/mL for
471 all strains of *Burkholderia*).

472 *Construction of pSC-rhadCas9, pAH-CTX1-rhadCas9, pAH-CTX1-rhadCas9-native, and dCas9*
473 *insertional mutants*

474 The endogenous *cas9* gene from *S. pyogenes* has low GC content (averaging 34.1%) and
475 subsequently poor codon usage for GC-rich organisms (http://www.kazusa.or.jp/codon/). The
476 nuclease-inactive variant (*dcas9*) was therefore codon optimized for *B. cenocepacia* by purchasing
477 the optimized gene in two fragments from IDT (2462 bp and 1849 bp, Supplemental Table 2), each
478 with 38 bp overlapping regions. Strong, rho-independent terminators were added following the
479 gene. The full-length gene (with terminal *Nde*I and *Hind*III cut sites) was synthesized by overlap-
480 extension PCR using Q5 polymerase with high GC buffer (NEB) and primers 979 and 987
481 (Supplemental Table 2). The first ten rounds of PCR were performed without primers to synthesize
482 the full-length product using the overlap regions; primers were added for the following 25 cycles.

483 The cycle parameters are as follows: 98°C for 30 sec, (98°C for 10 sec, 67.5°C for 20 sec, 72°C for
484 2.5 min)x10 cycles, 72°C for 5 min, 98°C for 30 sec, (98°C for 10 sec, 62.5°C for 20 sec,72 °C for
485 2.5 min)x25 cycles, 72°C for 10 min. The 4267 bp product was gel-purified (Qiagen) and
486 introduced into pSCrhaB2 by restriction cloning using *Nde*I and *Hind*III (NEB). The resulting
487 plasmid, pSC-rhadCas9, was transformed into *E. coli* DH5α, and trimethoprim-resistant colonies
488 were screened by colony PCR with primers 954 and 955. Triparental mating with *E.* coli
489 MM290/pRK2013 as a helper was performed as previously described [44].

490 To introduce the optimized *dcas9* into the mini-CTX1 insertion plasmid [24] serial restriction
491 cloning was used (Supplemental Figure 3A). Briefly, the rhamnose-inducible promoter from
492 pSC201 [45] was first PCR amplified with Q5 polymerase and primers 976 and 1071, containing
493 *Hind*III and *Spe*I restriction sites, respectively. This fragment was introduced into mini-CTX1, to
494 create pAH-CTX1-rha, and tetracycline-resistant *E. coli* DH5α were screened by colony PCR
495 using primers 957 and 1074. The fragment containing the dCas9 gene was PCR amplified as above,
496 but instead using primers 1072 and 1073, introducing *Spe*I and *Not*I restriction sites, respectively.
497 This fragment was introduced into pAH-CTX1-rha, to create pAH-CTX1-rhadCas9, and
498 tetracycline-resistant *E. coli* DH5α colonies were screened by colony PCR using primers 954 and
499 955.

500 The native (non codon-optimized) *dcas9* was also introduced into pAH-CTX1-rha. The
501 native *dcas9* and transcriptional terminators were PCR amplified from pdCas9-bacteria (Addgene
502 plasmid # 44249) with Q5 polymerase (NEB) using primers 1216 and 1217. The PCR product was
503 cloned into pAH-CTX1-rha (creating pAH-CTX1-rhadcas9-native) using *Not*I and *Spe*I restriction
504 sites then transformed into *E. coli* DH5α. Tetracycline-resistant colonies were screened by PCR
505 using primers 954 and 1218.

506 pAH-CTX1-rha, pAH-CTX1-rhadCas9, and pAH-CTX1-rhadCas9-native were
507 introduced into *Burkholderia* species by triparental mating using *E. coli* MM290/pRK2013 as a
508 helper as above. Tetracycline-resistant colonies were screened by colony PCR using primer 954
509 (for pAH-CTX1-rha) or 1075 (for pAH-CTX1-rhadCas9) or 1219 (for pAH-CTX1-rhadcas9-
510 native) and 1008 (for *B. cenocepacia*), 1167 (for *B. multivorans*), or 1168 (for *B. thailandensis*).

511 To remove the tetracycline resistance and integrase genes from the insertional mutants
512 constructed with pAH-CTX1-rhadCas9 and pAH-CTX1-rha (Supplemental Figure 3), the
513 Flannagan method [46] was used for *B. cenocepacia* K56-2, while the pFLPe system [47] was used for
514 *B. multivorans* ATCC 17616 and *B. thailandensis* E264. To remove the regions flanking the *FRT*
515 sites in *B. cenocepacia* K56-2, a fragment with 475 bp overlapping the upstream and downstream
516 regions of the *FRT* sites was designed and synthesized (IDT) with *Kpn*I and *Eco*RI restriction sites,
517 respectively. The fragment was ligated into pGPI-*Sce*I [46] via the *Kpn*I and *Eco*RI restriction sites,
518 creating pAH18, and transformed into *E. coli* SY327. Trimethoprim-resistant colonies were
519 screened for the insertion of the fragment with primer 153 and 154. pAH18 was introduced into
520 the mutant backgrounds via triparental mating, as described above. Trimethoprim-resistant K56-2
521 were screened by PCR for both possible integration orientations using primers 154 and 1126, or
522 153 and 1133. To initiate the second recombination, an *Sce*I-expressing plasmid is required;
523 however, the conventional plasmid, pDAI-*Sce*I, confers tetracycline resistance and could not be
524 selected for in the mutant background. Therefore, the tetracycline resistance cassette was removed
525 by digestion with *Age*I and *Xho*I. The chloramphenicol resistance gene *cat* was PCR amplified
526 from pKD3 [48] using primers 1084 and 1150, then ligated into the *Age*I and *Xho*I-digested pDAI-
527 *Sce*I backbone and transformed into *E. coli* DH5α, creating pAH25-*Sce*I. Chloramphenicol-
528 resistant colonies were screened with primers 1091 and 1150. pAH25-*Sce*I was introduced into the

529 mutant backgrounds by triparental mating as described above. Chloramphenicol-resistant colonies
530 were screened for sensitivity to trimethoprim (indicating excision of pAH18) and tetracycline
531 (indicating excision of the genes between the *FRT* sites), and then screened by PCR with primers
532 1126 and 1133, which bridge the excision.

533 The pFLPe system was used to remove the tetracycline resistance and integrase genes in
534 the dCas9 mutants in *B. multivorans* ATCC 17616 and *B. thailandensis* E264. Triparental mating
535 to introduce pFLPe4 into the strains was performed as for K56-2 above, except 0.2% rhamnose
536 was added to the mating and antibiotic selection plates. Tetracycline-sensitive colonies were
537 screened by PCR using primers 957 and 1194 (for *B. multivorans*) or 1195 (for *B. thailandensis*).
538 pFLPe4 has a temperature-sensitive origin of replication; therefore, mutants were grown overnight
539 in LB without antibiotics at 37°C. Single colonies were then tested for kanamycin sensitivity and
540 then by colony PCR for pFLPe4 using primers 1128 and 1129.

541 *Design and construction of the sgRNA-expressing plasmids*

542 PAM sequences closest to the 5' end of the transcription start site (TSS) were first
543 identified on both the non-template and template strands. We extracted 20-23 nucleotides adjacent
544 to the PAM sequence to design the base-pairing region of the sgRNAs in the following format: 5'-
545 CCN-$N_{(20-23)}$-3' for targeting the non-template strand and 5'-$N_{(20-23)}$-NGG-3' for the template
546 strand. To score the specificity and identify off-target binding sites, the 5' end of the 20-23nt
547 variable base-pairing sequences were trimmed one base at a time and the remaining base-pairing
548 region was searched against the appropriate organism's reference genome. This was repeated until
549 only 10 nt were used as a search query. Potential sgRNAs were discarded if off-target sites were
550 discovered in this manner.

551 The expression vector pSCrhaB2 [25] was chosen as the method of sgRNA expression due
552 to the broad host range of the pBBR1 origin of replication. The sgRNA cassette from pgRNA-
553 bacteria [9] (Addgene plasmid # 44251) was introduced into pSCrhaB2 by restriction cloning with
554 *Eco*RI and *Hind*III (NEB) to create pSCrhaB2-sgRNA. To remove *rhaS* and *rhaR*, inverse PCR
555 was performed using Q5 polymerase (NEB) and primers 847 and 1025. The resulting fragment
556 was ligated by blunt-end ligation using 1 μL of PCR product incubated with 0.5 μL *Dpn*I, 0.5 μL
557 T4 polynucleotide kinase, and 0.5 μL T4 ligase (NEB) with quick ligation buffer (NEB) at 37°C
558 for 30 minutes. The resulting plasmid, pSCB2-sgRNA, was screened using primers 781 and 848,
559 which span the ligated junction. Individual sgRNAs were introduced into pSCB2-sgRNA using
560 inverse PCR as previously described [9] (Supplemental Table 3).

561 *Construction of insertional mutants K56-2 fliF::pAH26 and K56-2 phbC::pAH27*

562 Inactivation of *fliF* was performed with the mutagenesis system of Flannagan et al. [49].
563 Briefly, a 322 bp internal fragment of *fliF* was PCR amplified from the K56-2 genome using
564 primers 1156 and 1157 and Q5 polymerase (NEB). The fragment and pGPΩ-Tp were double
565 digested with *Kpn*I and *Eco*RI (NEB) and ligated with T4 ligase (NEB). The resulting plasmid,
566 pAH26, was electroporated into *E. coli* SY327, and trimethoprim-resistant colonies were screened
567 by colony PCR for the *fliF* fragment. Triparental matings were performed as above. Trimethoprim-
568 resistant exconjugants, were screened by motility assay (below).

569 Inactivation of *phbC* (WQ49_RS30385) was performed as for *fliF*. Briefly, a 328 bp
570 internal fragment of *phbC* was PCR amplified from the K56-2 genome using primers 1196 and
571 1197 and Q5 polymerase (NEB). The plasmid, pAH27, created from ligating the fragment into
572 pGPΩ-Tp using *Kpn*I and *Eco*RI (NEB) restriction sites, was electroporated into *E. coli* SY327
573 and trimethoprim-resistant colonies were screened by colony PCR for the *phbC* fragment.

574 Triparental matings were performed as above, and trimethoprim-resistant exconjugants were
575 screened by staining for polyhydroxyalkanoate granule accumulation (below).

576 *Assays for integration efficiency and stability of the mini-CTX1-based system*

577 To assess integration efficiency, triparental matings were started as above. However, after
578 the mating on LB agar, the pellicles were serially diluted and plated for CFU/mL on LB agar with
579 50 µg/mL gentamicin and LB agar with 50 µg/mL tetracycline and 50 µg/mL gentamicin.

580 To assess stability of the integration, cultures of the dCas9 mutants (containing the
581 tetracycline resistance cassette) were serial passaged over 4 days without antibiotics. Each day, a
582 fresh culture was started with a 1:2500 dilution of the previous day's stationary phase culture. In
583 addition, the cultures were serially diluted and plated for CFU/mL on LB agar without antibiotics
584 and LB agar with 50 µg/mL tetracycline.

585 *Growth assay with phenylacetic acid as the sole carbon source*

586 Overnight cultures, started from isolated colonies, of the appropriate strains were washed
587 at 4000 xg for 4 minutes and resuspended in PBS (2.7 mM KCl, 136.9 mM NaCl, 1.5 mM KH_2PO_4,
588 8.9 mM Na_2HPO_4, pH 7.4) to remove growth medium. The OD_{600nm} of the cultures was normalized
589 to 0.01 in M9 medium supplemented with 5 mM phenylacetic acid, 100 µg/mL trimethoprim, and
590 0.2% rhamnose as required. The culture was added to wells of a 96-well plate and incubated with
591 continuous shaking at 37°C (*B. cenocepacia* K56-2) or 30°C for *B. multivorans* ATCC 17616 and
592 *B. thailandensis* E264). The OD_{600nm} of the cultures was measured after 24 hours for *B.*
593 *cenocepacia* K56-2 and *B. multivorans* ATCC 17616, or 48 hours for *B. thailandensis* E264.

594

595 *Fluorescent microscopy and polyhydroxyalkanoate granule detection*

596 Overnight cultures of the appropriate strains with or without rhamnose were first washed
597 to remove growth medium and resuspended in PBS. Cells were fixed in 3.7% formaldehyde + 1%
598 methanol at room temperature for 10 minutes (*B. cenocepacia* K56-2) or 20 minutes (*B.*
599 *multivorans* ATCC 17616 and *B. thailandensis* E264) then quenched by the addition of an equal
600 volume of 0.5 M glycine. The cells were washed and resuspended in PBS with 0.5 μg/mL Nile
601 Red (Carbosynth) and stained at room temperature in the dark for 20 minutes, after which the cells
602 were washed to remove excess stain and resuspended in PBS. The cells were mounted on 1.5%
603 agarose pads and imaged by fluorescence microscopy at 1000x total magnification on an upright
604 AxioImager Z1 (Zeiss). Nile Red was excited at 546/12 nm and detected at 607/33 nm.

605 *Plate-based motility assay*

606 Assays were performed as previously described [50], with some modifications. Briefly,
607 strains were grown on LB agar with the appropriate antibiotics and single colonies were stab-
608 inoculated into motility medium consisting of nutrient broth (Difco) with 0.3% agar. Medium was
609 supplemented with rhamnose (Sigma) as appropriate. Plates were incubated right-side up for 22
610 hours at 37°C.

611 *Flagellum staining*

612 Staining was performed as previously described [50]. Briefly, an overnight culture was rested
613 statically at room temperature for 20 minutes. Gently, a 1 in 10 dilution was prepared in water and
614 rested statically for a further 20 minutes. A small drop of the diluted culture was placed on a clean
615 glass slide and rested for 20 minutes. A coverglass was gently applied and one side was flooded
616 with Ryu flagellum stain (Remel), then allowed to dry for 2 hours at room temperature. Slides

617 were observed by light microscopy at 1000x total magnification on an upright AxioImager Z1
618 (Zeiss).

619 *SDS-PAGE and Immunoblotting*

620 Cells from an overnight culture were subcultured into fresh medium and grown at 37°C
621 (30°C for *B. thailandensis*) to an OD_{600nm} of 0.4, then exposed to various concentrations of
622 rhamnose for 3 hours. Soluble protein was isolated first by sonicating the cells in TNG Buffer (100
623 mM Tris-HCl, 150 mM NaCl, 10% glycerol, pH 7.4) then by centrifugation at 15 000g for 20
624 minutes. Following boiling denaturation in SDS loading buffer (50 mM Tris-HCl, 2% SDS, 0.2%
625 bromophenol blue, 20% glycerol, 100 mM DTT, pH 6.8), samples were run on an 8% Tris/glycine
626 gel. To ensure equal loading, 20 µg protein was loaded per well (as determined by NanoDrop) and
627 gels were run in duplicate (one for immunoblot, and another for Coomassie staining). Protein was
628 transferred by iBlot to a PVDF membrane, blocked in 5% skim milk-TBST (150 mM NaCl, 10
629 mM Tris-HCl, 0.5% Tween-20, pH 7.5) at room temperature for 1 hour, then probed with a 1:2
630 000 dilution of primary α-Cas9 antibody (ThermoFisher 10C11-A12) in 5% skim milk-TBST
631 overnight at 4°C. Following washes, the blot was probed with a 1:20 000 dilution of secondary
632 antibody linked to alkaline phosphatase (ThermoFisher G-21060) in 5% skim milk-TBST for 1
633 hour at room temperature. Protein was detected by incubation with a solution of NBT/BCIP
634 (Roche) as per the manufacturer's protocol.

635 *RNA extraction and Reverse Transcription quantitative PCR (RT-qPCR) analysis*

636 Cells from an overnight culture were subcultured at an OD_{600nm} of 0.01 into fresh medium
637 with antibiotic and rhamnose, as necessary, and grown for 8 hours. Cells were harvested by
638 centrifugation (3 minutes at 4600xg) and pellets were stored at -80°C until RNA extraction. RNA

639 was purified and DNAse treated using the Ribopure bacteria kit (Ambion) with extended DNAse
640 treatement (2 hours). RNA quality was verified by running on a 2% agarose gel. cDNA was
641 synthesized with the iScript Reverse Transcriptase kit (Bio-Rad) and qPCR was performed using
642 iQ SYBR Green mastermix (Bio-rad) on a CFX96 Touch Real-Time PCR Detection System (Bio-
643 Rad). Primer efficiency was determined for each primer set and efficiencies between 95% and
644 105% were deemed acceptable. Data was analyzed using the comparative C_T method [51,52]. Genes
645 were normalized to a commonly used reference gene, the RNA polymerase sigma factor *sigE*
646 (BCAM0918) [53,54].

647 *Plasmid availability*

648 The following plasmids have been deposited to Addgene for distribution: pAH-CTX1-rha
649 (#129390), pAH-CTX1-rhadCas9 (#129391), pAH-CTX1-rhadCas9-native (#129392), pAH25-
650 SceI (#129389), pSCB2-sgRNA (#129463), pgRNA-guideless (#129464), and pgRNA-non-target
651 (#129465).

652 **Acknowledgements**

653 This work was financially supported by grants from the Cystic Fibrosis Foundation, Cystic
654 Fibrosis Canada, and the Natural Sciences and Engineering Research Council of Canada (NSERC)
655 to STC; AMH was supported by grants from the Canadian Institutes of Health Research (CIHR)
656 and Cystic Fibrosis Canada.

657 The authors are grateful to Eric Déziel from the Institut National de la Recherche
658 Scientifique – Institut Armand-Frappier for providing the miniCTX1 integration vector.

659

660 **Conflict of Interest Statement**

661 The authors declare no conflict of interest.

662

663 **References**

664 (1) Eberl, L., and Vandamme, P. (2016) Members of the genus *Burkholderia*: good and bad
665 guys. *F1000Research 5*, 1007.
666 (2) Depoorter, E., Bull, M. J., Peeters, C., Coenye, T., Vandamme, P., and Mahenthiralingam, E.
667 (2016) *Burkholderia*: an update on taxonomy and biotechnological potential as antibiotic
668 producers. *Appl. Microbiol. Biotechnol. 100*, 5215–5229.
669 (3) Mahenthiralingam, E., Urban, T. A., and Goldberg, J. B. (2005) The multifarious,
670 multireplicon *Burkholderia cepacia* complex. *Nat. Rev. Microbiol. 3*, 144–156.
671 (4) Kenna, D. T. D., Lilley, D., Coward, A., Martin, K., Perry, C., Pike, R., Hill, R., and Turton,
672 J. F. (2017) Prevalence of *Burkholderia* species, including members of *Burkholderia cepacia*
673 complex, among UK cystic and non-cystic fibrosis patients. *J. Med. Microbiol. 66*, 490–501.
674 (5) Howe, C., Sampath, A., and Spotnitz, M. (1971) The *pseudomallei* group: a review. *J. Infect.*
675 *Dis. 124*, 598–606.
676 (6) Nally, E., Groah, S. L., Pérez-Losada, M., Caldovic, L., Ljungberg, I., Chandel, N. J.,
677 Sprague, B., Hsieh, M. H., and Pohl, H. G. (2018) Identification of *Burkholderia fungorum* in the
678 urine of an individual with spinal cord injury and augmentation cystoplasty using 16S
679 sequencing: copathogen or innocent bystander? *Spinal Cord Ser. Cases 4*, 85.
680 (7) Rhodes, K. A., and Schweizer, H. P. (2016) Antibiotic resistance in *Burkholderia* species.
681 *Drug Resist. Updat. 28*, 82–90.
682 (8) Judson, N., and Mekalanos, J. J. (2000) TnAraOut, a transposon-based approach to identify
683 and characterize essential bacterial genes. *Nat Biotechnol 18*, 740–745.
684 (9) Qi, L. S., Larson, M. H., Gilbert, L. A., Doudna, J. A., Weissman, J. S., Arkin, A. P., and
685 Lim, W. A. (2013) Repurposing CRISPR as an RNA-guided platform for sequence-specific
686 control of gene expression. *Cell 152*, 1173–1183.
687 (10) Cho, S. W., Kim, S., Kim, J. M., and Kim, J.-S. (2013) Targeted genome engineering in
688 human cells with the Cas9 RNA-guided endonuclease. *Nat. Biotechnol. 31*, 230–232.
689 (11) Croteau, F. R., Rousseau, G. M., and Moineau, S. (2018) The CRISPR-Cas system: beyond
690 genome editing. *Med. Sci. MS 34*, 813–819.
691 (12) Kim, S. K., Han, G. H., Seong, W., Kim, H., Kim, S.-W., Lee, D.-H., and Lee, S.-G. (2016)
692 CRISPR interference-guided balancing of a biosynthetic mevalonate pathway increases
693 terpenoid production. *Metab. Eng. 38*, 228–240.
694 (13) Tan, S. Z., Reisch, C. R., and Prather, K. L. J. (2018) A robust CRISPRi gene repression
695 system in *Pseudomonas*. *J. Bacteriol. 200*, e00575-17.
696 (14) Yao, L., Cengic, I., Anfelt, J., and Hudson, E. P. (2016) Multiple gene repression in
697 cyanobacteria using CRISPRi. *ACS Synth. Biol. 5*, 207–212.
698 (15) Zhang, B., Liu, Z.-Q., Liu, C., and Zheng, Y.-G. (2016) Application of CRISPRi in
699 *Corynebacterium glutamicum* for shikimic acid production. *Biotechnol. Lett. 38*, 2153–2161.

700 (16) Lee, H. H., Ostrov, N., Wong, B. G., Gold, M. A., Khalil, A. S., and Church, G. M. (2019)
701 Functional genomics of the rapidly replicating bacterium *Vibrio natriegens* by CRISPRi. *Nat.*
702 *Microbiol. 4,* 1105-1113
703 (17) Liu, X., Gallay, C., Kjos, M., Domenech, A., Slager, J., van Kessel, S. P., Knoops, K., Sorg,
704 R. A., Zhang, J.-R., and Veening, J.-W. (2017) High-throughput CRISPRi phenotyping identifies
705 new essential genes in *Streptococcus pneumoniae*. *Mol. Syst. Biol. 13*, 931.
706 (18) Peters, J. M., Colavin, A., Shi, H., Czarny, T. L., Larson, M. H., Wong, S., Hawkins, J. S.,
707 Lu, C. H., Koo, B. M., Marta, E., Shiver, A. L., Whitehead, E. H., Weissman, J. S., Brown, E.
708 D., Qi, L. S., Huang, K. C., and Gross, C. A. (2016) A comprehensive, CRISPR-based functional
709 analysis of essential genes in bacteria. *Cell 165*, 1493–1506.
710 (19) Cui, L., Vigouroux, A., Rousset, F., Varet, H., Khanna, V., and Bikard, D. (2018) A
711 CRISPRi screen in *E. coli* reveals sequence-specific toxicity of dCas9. *Nat. Commun. 9*, 1912.
712 (20) Choi, K.-H., and Schweizer, H. P. (2006) Mini-Tn7 insertion in bacteria with single attTn*7*
713 sites: example *Pseudomonas aeruginosa*. *Nat. Protoc. 1*, 153–161.
714 (21) Choi, K. H., Gaynor, J. B., White, K. G., Lopez, C., Bosio, C. M., Karkhoff-Schweizer, R.
715 R., and Schweizer, H. P. (2005) A Tn*7*-based broad-range bacterial cloning and expression
716 system. *Nat.Methods 2*, 443–448.
717 (22) Peters, J. M., Koo, B.-M., Patino, R., Heussler, G. E., Hearne, C. C., Qu, J., Inclan, Y. F.,
718 Hawkins, J. S., Lu, C. H. S., Silvis, M. R., Harden, M. M., Osadnik, H., Peters, J. E., Engel, J.
719 N., Dutton, R. J., Grossman, A. D., Gross, C. A., and Rosenberg, O. S. (2019) Enabling genetic
720 analysis of diverse bacteria with Mobile-CRISPRi. *Nat. Microbiol. 4*, 244.
721 (23) Choi, K. H., DeShazer, D., and Schweizer, H. P. (2006) Mini-Tn7 insertion in bacteria with
722 multiple *glmS*-linked attTn7 sites: example *Burkholderia mallei* ATCC 23344. *Nat. Protoc. 1*,
723 162–169.
724 (24) Hoang, T. T., Kutchma, A. J., Becher, A., and Schweizer, H. P. (2000) Integration-
725 proficient plasmids for *Pseudomonas aeruginosa*: site-specific integration and use for
726 engineering of reporter and expression strains. *Plasmid 43*, 59–72.
727 (25) Cardona, S. T., and Valvano, M. A. (2005) An expression vector containing a rhamnose-
728 inducible promoter provides tightly regulated gene expression in *Burkholderia cenocepacia*.
729 *Plasmid 54*, 219–228.
730 (26) Rock, J. M., Hopkins, F. F., Chavez, A., Diallo, M., Chase, M. R., Gerrick, E. R., Pritchard,
731 J. R., Church, G. M., Rubin, E. J., Sassetti, C. M., Schnappinger, D., and Fortune, S. M. (2017)
732 Programmable transcriptional repression in mycobacteria using an orthogonal CRISPR
733 interference platform. *Nat. Microbiol. 2*, 16274.
734 (27) Choudhary, E., Thakur, P., Pareek, M., and Agarwal, N. (2015) Gene silencing by CRISPR
735 interference in mycobacteria. *Nat. Commun. 6*, 6267.
736 (28) Teufel, R., Mascaraque, V., Ismail, W., Voss, M., Perera, J., Eisenreich, W., Haehnel, W.,
737 and Fuchs, G. (2010) Bacterial phenylalanine and phenylacetate catabolic pathway revealed.
738 *Proc. Natl. Acad. Sci. U. S. A. 107*, 14390–14395.
739 (29) Pribytkova, T., Lightly, T. J., Kumar, B., Bernier, S. P., Sorensen, J. L., Surette, M. G., and
740 Cardona, S. T. (2014) The attenuated virulence of a *Burkholderia cenocepacia paaABCDE*
741 mutant is due to inhibition of quorum sensing by release of phenylacetic acid. *Mol. Microbiol.*
742 *94*, 522–536.
743 (30) Bikard, D., Jiang, W., Samai, P., Hochschild, A., Zhang, F., and Marraffini, L. A. (2013)
744 Programmable repression and activation of bacterial gene expression using an engineered
745 CRISPR-Cas system. *Nucleic Acids Res. 41*, 7429–7437.

746 (31) Francis, N. R., Irikura, V. M., Yamaguchi, S., DeRosier, D. J., and Macnab, R. M. (1992)
747 Localization of the *Salmonella typhimurium* flagellar switch protein FliG to the cytoplasmic M-
748 ring face of the basal body. *Proc. Natl. Acad. Sci. 89*, 6304–6308.
749 (32) Yang, P., Zhang, M., and Elsas, J. D. van. (2017) Role of flagella and type four pili in the
750 co-migration of *Burkholderia terrae* BS001 with fungal hyphae through soil. *Sci. Rep. 7*, 2997.
751 (33) Komatsu, H., Hayashi, F., Sasa, M., Shikata, K., Yamaguchi, S., Namba, K., and Oosawa,
752 K. (2016) Genetic analysis of revertants isolated from the rod-fragile fliF mutant of *Salmonella*.
753 *Biophys. Physicobiology 13*, 13–25.
754 (34) Tomich, M., Herfst, C. A., Golden, J. W., and Mohr, C. D. (2002) Role of flagella in host
755 cell invasion by *Burkholderia cepacia*. *Infect. Immun. 70*, 1799–1806.
756 (35) Mao, D., Bushin, L. B., Moon, K., Wu, Y., and Seyedsayamdost, M. R. (2017) Discovery of
757 *scmR* as a global regulator of secondary metabolism and virulence in *Burkholderia thailandensis*
758 E264. *Proc. Natl. Acad. Sci. U. S. A. 114*, E2920–E2928.
759 (36) Funston, S. J., Tsaousi, K., Smyth, T. J., Twigg, M. S., Marchant, R., and Banat, I. M.
760 (2017) Enhanced rhamnolipid production in *Burkholderia thailandensis* transposon knockout
761 strains deficient in polyhydroxyalkanoate (PHA) synthesis. *Appl. Microbiol. Biotechnol. 101*,
762 8443–8454.
763 (37) Chapalain, A., Groleau, M.-C., Le Guillouzer, S., Miomandre, A., Vial, L., Milot, S., and
764 Déziel, E. (2017) Interplay between 4-hydroxy-3-methyl-2-alkylquinoline and N-acyl-
765 homoserine lactone signaling in a *Burkholderia cepacia* complex clinical strain. *Front.*
766 *Microbiol. 8*, 1021.
767 (38) Le Guillouzer, S., Groleau, M.-C., and Déziel, E. (2017) The complex quorum-sensing
768 circuitry of *Burkholderia thailandensis* is both hierarchically and homeostatically organized.
769 *mBio 8*.
770 (39) Cho, S., Choe, D., Lee, E., Kim, S. C., Palsson, B., and Cho, B.-K. (2018) High-level dCas9
771 expression induces abnormal cell morphology in *Escherichia coli*. *ACS Synth. Biol. 7*, 1085-
772 1094.
773 (40) Jones, D. L., Leroy, P., Unoson, C., Fange, D., Ćurić, V., Lawson, M. J., and Elf, J. (2017)
774 Kinetics of dCas9 target search in *Escherichia coli*. *Science 357*, 1420–1424.
775 (41) Guo, J., Wang, T., Guan, C., Liu, B., Luo, C., Xie, Z., Zhang, C., and Xing, X.-H. (2018)
776 Improved sgRNA design in bacteria via genome-wide activity profiling. *Nucleic Acids Res. 46*,
777 7052–7069.
778 (42) Josephs, E. A., Kocak, D. D., Fitzgibbon, C. J., McMenemy, J., Gersbach, C. A., and
779 Marszalek, P. E. (2015) Structure and specificity of the RNA-guided endonuclease Cas9 during
780 DNA interrogation, target binding and cleavage. *Nucleic Acids Res. 43*, 8924–8941.
781 (43) Siegele, D. A., and Hu, J. C. (1997) Gene expression from plasmids containing the araBAD
782 promoter at subsaturating inducer concentrations represents mixed populations. *Proc Natl Acad*
783 *Sci U A 94*, 8168–72.
784 (44) Hogan, A. M., Scoffone, V. C., Makarov, V., Gislason, A. S., Tesfu, H., Stietz, M. S.,
785 Brassinga, A. K. C., Domaratzki, M., Li, X., Azzalin, A., Biggiogera, M., Riabova, O.,
786 Monakhova, N., Chiarelli, L. R., Riccardi, G., Buroni, S., and Cardona, S. T. (2018) Competitive
787 fitness of essential gene knockdowns reveals a broad-spectrum antibacterial inhibitor of the cell
788 division protein FtsZ. *Antimicrob. Agents Chemother. 62*, e01231-18
789 (45) Ortega, X. P., Cardona, S. T., Brown, A. R., Loutet, S. A., Flannagan, R. S., Campopiano,
790 D. J., Govan, J. R., and Valvano, M. A. (2007) A putative gene cluster for aminoarabinose
791 biosynthesis is essential for *Burkholderia cenocepacia* viability. *J. Bacteriol. 189*, 3639–3644.

792 (46) Flannagan, R. S., Linn, T., and Valvano, M. A. (2008) A system for the construction of
793 targeted unmarked gene deletions in the genus *Burkholderia*. *Environ. Microbiol. 10*, 1652–
794 1660.
795 (47) Choi, K. H., Mima, T., Casart, Y., Rholl, D., Kumar, A., Beacham, I. R., and Schweizer, H.
796 P. (2008) Genetic tools for select-agent-compliant manipulation of *Burkholderia pseudomallei*.
797 *Appl. Environ. Microbiol. 74*, 1064–1075.
798 (48) Datsenko, K. A., and Wanner, B. L. (2000) One-step inactivation of chromosomal genes in
799 *Escherichia coli* K-12 using PCR products. *Proc Natl Acad Sci U A 97*, 6640–6645.
800 (49) Flannagan, R. S., Aubert, D., Kooi, C., Sokol, P. A., and Valvano, M. A. (2007)
801 *Burkholderia cenocepacia* requires a periplasmic HtrA protease for growth under thermal and
802 osmotic stress and for survival *in vivo*. *Infect. Immun. 75*, 1679–1689.
803 (50) Kumar, B., and Cardona, S. T. (2016) Synthetic cystic fibrosis sputum medium regulates
804 flagellar biosynthesis through the *flhF* gene in *Burkholderia cenocepacia*. *Front. Cell. Infect.*
805 *Microbiol. 6*, 65.
806 (51) Livak, K. J., and Schmittgen, T. D. (2001) Analysis of relative gene expression data using
807 real-time quantitative PCR and the 2(-Delta Delta C(T)) Method. *Methods 25*, 402–408.
808 (52) Schmittgen, T. D., and Livak, K. J. (2008) Analyzing real-time PCR data by the
809 comparative C(T) method. *Nat. Protoc. 3*, 1101–1108.
810 (53) O'Grady, E. P., Viteri, D. F., Malott, R. J., and Sokol, P. A. (2009) Reciprocal regulation by
811 the CepIR and CciIR quorum sensing systems in *Burkholderia cenocepacia*. *BMC Genomics 10*.
812 (54) Wong, Y.-C., Abd El Ghany, M., Ghazzali, R. N. M., Yap, S.-J., Hoh, C.-C., Pain, A., and
813 Nathan, S. (2018) Genetic determinants associated with *in vivo* survival of *Burkholderia*
814 *cenocepacia* in the *Caenorhabditis elegans* model. *Front. Microbiol. 9*, 1118.